Published in final edited form as:
Neurobiol Learn Mem. 2013 March ; 101: 75–84. doi:10.1016/j.nlm.2013.01.006.

Tone-detection training enhances spectral integration mediated by intracortical pathways in primary auditory cortex

Fei Guo[1,2,*], **Irakli Intskirveli**[1,*], **David T. Blake**[3], and **Raju Metherate**[1]

[1]Department of Neurobiology and Behavior and Center for Hearing Research, University of California, Irvine, California 92697, USA

[2]School of Life Science, Key Laboratory of Brain Functional Genomics, Ministry of Education, East China Normal University, Shanghai 200062, China

[3]Brain and Behavior Discovery Institute, Georgia Health Sciences University, CB-3702, Augusta, GA 30912, USA

Abstract

Auditory-cued behavioral training can alter neural circuits in primary auditory cortex (A1), but the mechanisms and consequences of experience-dependent cortical plasticity are not fully understood. To address this issue, we trained adult rats to detect a 5 kHz target in order to receive a food reward. After 14 days training we identified three locations within A1: i) the region representing the characteristic frequency (CF) 5 kHz, ii) a nearby region with CF ~10 kHz, and iii) a more distant region with CF ~20 kHz. In order to compare functional connectivity in A1 near to, vs. far from, the representation of the target frequency, we placed a 16-channel multiprobe in middle- (~10 kHz) and high- (~20 kHz) CF regions and obtained current-source density (CSD) profiles evoked by a range of tone stimuli (CF ± 1–3 octaves in quarter-octave steps). Our aim was to construct "CSD receptive fields" (CSD RFs) in order to determine the laminar and spectral profile of tone-evoked current sinks, and infer changes to thalamocortical and intracortical inputs. Behavioral training altered CSD RFs at the 10 kHz, but not 20 kHz, site relative to CSD RFs in untrained control animals. At the 10 kHz site, current sinks evoked by the target frequency were enhanced in layer 2/3, but the initial current sink in layer 4 was not altered. The results imply training-induced plasticity along intracortical pathways connecting the target representation with nearby cortical regions. Finally, we related behavioral performance (sensitivity index, d′) to CSD responses in individual animals, and found a significant correlation between the development of d′ over training and the amplitude of the target-evoked current sink in layer 2/3. The results suggest that plasticity along intracortical pathways is important for auditory learning.

Keywords

auditory cortex; rat; plasticity; behavior; current-source density; thalamocortical; learning

Corresponding Author: Raju Metherate, Ph.D., University of California, Irvine, 2205 McGaugh Hall, Irvine, CA 92697-4550, (949) 824-6141, fax: (949) 824-2447, raju.metherate@uci.edu.
*These authors contributed equally.

1. Introduction

A1 is organized topographically by frequency, yet its organization can be modified by auditory experience (Edeline, 2003; Irvine, 2007; Scheich, Brechmann, Brosch, Budinger, & Ohl, 2007; Weinberger, 2007). For example, frequency-discrimination training in adult monkeys can alter the tonotopic map of CF to increase the area devoted to frequencies relevant for training (Recanzone, Schreiner, & Merzenich, 1993). Similarly, single and multi-unit recordings show that frequency RFs can become biased towards stimuli that acquire behavioral significance during training (Bakin & Weinberger, 1990; Fritz, Shamma, Elhilali, & Klein, 2003), a phenomenon that presumably underlies frequency-specific plasticity of tonotopic maps. Studies have shown that training procedures can alter physiological response properties in ways that are related to the specific information acquired, implying that the nature of cortical plasticity depends on task demands (Bieszczad & Weinberger, 2010a; Fritz, Elhilali, & Shamma, 2005; Polley, Steinberg, & Merzenich, 2006; Scheich, et al., 2007). In some cases, the extent of map expansion correlates with improvements in behavioral performance and resistance to behavioral extinction, suggesting that the degree of plasticity may determine the strength of learning (Bieszczad & Weinberger, 2010b; Polley, et al., 2006; Recanzone, et al., 1993; Rutkowski & Weinberger, 2005). However, other studies found that improvements in auditory perception can occur in the absence of significant plasticity of tonotopy in A1 (Brown, Irvine, & Park, 2004). It appears that auditory training can lead to specific and selective changes in neuronal circuit properties in A1 that underlie improvements in behavioral performance; these changes may or may not produce changes in tonotopic maps.

Although a number of studies have demonstrated learning-related plasticity in A1, fewer have examined cellular and molecular mechanisms (Carpenter-Hyland, Plummer, Vazdarjanova, & Blake, 2010; Guo et al., 2012). Even the locus of plasticity is not fully established, since changes observed in A1 may not originate there but instead could be relayed from subcortical structures (Ma & Suga, 2009). One approach to better understand the nature and locus of plasticity in A1 is to determine the laminar profile of physiological changes using tone-evoked CSD analysis. Because CSD analysis can help to distinguish thalamocortical from intracortical contributions to evoked responses (Happel, Jeschke, & Ohl, 2010; Intskirveli & Metherate, 2012; H. Kawai, Lazar, & Metherate, 2007; H. D. Kawai, Kang, & Metherate, 2011), it can be used to address whether plasticity originates within A1 or exists already in thalamic inputs.

Thus, to examine intracortical and subcortical contributions to plasticity we applied CSD analysis to learning-induced plasticity in A1. The results show that tone-detection training altered responses at a cortical site with CF ~10 kHz (~1 octave above the target), producing plasticity of tone-evoked responses within cortical layers 2–4. At this cortical site, altered target-evoked current sinks in layer 2/3 implicate intracortical neural circuits, and altered sinks in layer 4 also were more likely associated with intracortical, rather than thalamocortical, synapses. Importantly, in individual animals the magnitude of the target-evoked intracortical, but not thalamocortical, responses correlated with the development of learned behavior. These results help elucidate the origins of learning-related plasticity in A1.

2. Materials and Methods

2.1 Animals

Male Sprague-Dawley rats 55–58 days old were obtained from a commercial breeder (Charles River). All animal procedures were approved by the Institutional Animal Care and Use Committee of the University of California, Irvine.

2.2. Operant training

Animals were handled daily for a minimum of three days before the start of behavioral training. Prior to tone-detection training, rats underwent behavioral shaping to nose poke for food pellets (45 mg pellets, Bio-Serv) using a operant chamber placed inside an acoustically shielded box (Habitest, Coulbourn Instruments). The nose poke and pellet dispenser were controlled using custom software (LabView, National Instruments). The animal was trained to hold a nose poke for progressively longer durations, up to 800 ms, in order to receive a food pellet. Most of each animal's daily allotment of food was obtained during training sessions, and each session was terminated when the animal earned ~200 pellets, or after one hour. Upon return to the home cage, each animal was given an additional 4 g of food. On non-training days (weekends) animals received 16 g of food. Animals had unlimited access to water, were weighed daily, and during training remained at ~85–95% of their pre-training weight. Nose-poke shaping continued for a minimum of 10 days until reliable 800 ms holds were maintained for three consecutive days, at which point tone-detection training began. In that task, animals were required to release the nose poke upon presentation of a 5 kHz target tone (50 dB, 25 ms) produced by a speaker (FF-1, Tucker Davis Technologies) located on the ceiling of the acoustic chamber (calibration performed using a microphone positioned near the floor of the chamber). The target tone was presented randomly at one of two times, either 400 ms or 800 ms after initiation of the nose poke. In either case, the nose poke had to be withdrawn within 400 ms of tone onset to be rewarded. Performance was evaluated using the sensitivity index (d') from signal detection theory, which is equal to the z-score difference between hit and false alarm rates. Thus, the behavioral metric (d') compares the animal's responses over the 400–800 ms window after nose-poke initiation. Some responses within this window follow tones at 400 ms (hits), and others do not follow a tone (false alarms, on trials that would have presented a tone at 800 ms). The probability of hits and false alarms is determined, and d' calculated as the z-score difference between the two probabilities (z-scores determined using the norminv() function in Matlab), i.e., $d' = z(\text{hits}) - z(\text{false alarms})$.

Surgical procedure

Rats were anesthetized with urethane (0.7 g/kg i.p., Sigma) and xylazine (13 mg/kg i.p., Phoenix Pharmaceutics), placed in a sound-attenuating chamber (AC-3, IAC) and maintained at 37 deg. C. Anesthesia was supplemented at ~1 h intervals in order to maintain lack of reflex response to tail or paw pinch, with urethane (0.13 g/kg) and xylazine (1.3 mg/kg) administered via a catheter to avoid movement. The head was secured in a stereotaxic frame (model 923, Kopf Instruments) using blunt earbars. After a midline incision, the skull was cleared and secured using a custom head holder fixed onto the skull. A craniotomy was performed over the right temporal cortex and the exposed brain was kept moist with warmed saline. Subsequently, the earbars were removed to permit acoustic stimulation.

Electrophysiology and acoustic stimulation

For mapping A1, multiunit activity was recorded using a tungsten electrode. For CSD profiles, local field potentials (LFPs) were recorded using a 16-channel silicon multiprobe (~2–3 Mω at 1 kHz for each 177 μm^2 recording site, 100 μm separation between recording sites; NeuroNexus Technologies), with the multiprobe advanced into the cortex until the first channel was just visible at the cortical surface. LFPs were filtered and amplified (1 Hz to 10 kHz, AI-401 or AI-405, CyberAmp 380; Axon Instruments), digitized and stored on a computer (Macintosh running AxoGraph software). Acoustic stimuli were digitally synthesized and controlled using MALab (Kaiser Instruments) and a computer (Macintosh) and delivered through a speaker (ES-1 or FF-1 with ED-1 driver, Tucker-Davis Technologies) positioned ~3 cm in front of the left ear. For calibration (sound pressure level, SPL, in dB re: 20 μPa) a model 4939 microphone and Nexus amplifier (Brüel and Kjaer)

was positioned in place of the animal at the location of the left earbar tip. Tones were 100 ms in duration with 5 ms linear rise and fall ramps; range 1–40 kHz and −10 dB to 70 dB SPL. For data collection, stimuli were delivered at a rate of 1/s in sets of 25 trials.

Laminar CSD analysis

Tone-evoked CSD profiles were constructed and analyzed off-line as described previously (Intskirveli & Metherate, 2012; Kaur, Rose, Lazar, Liang, & Metherate, 2005; H. D. Kawai, et al., 2011). One-dimensional CSD profiles are the second spatial derivative of the LFP laminar profile (Muller-Preuss & Mitzdorf, 1984); conventionally, a current sink implies the location of underlying net synaptic excitation. The onset of a tone-evoked current sink was defined as the time at which the response crossed a threshold 2 standard deviations above baseline. The middle-layer sink with shortest onset latency (typically 500–700 μm depth) was designated the initial sink and assigned to "layer 4" for purposes of averaging across animals, and its initial amplitude considered a reflection of monosynaptic thalamocortical input (Intskirveli & Metherate, 2012; H. D. Kawai, et al., 2011); see Discussion section 4.1.

Statistical analyses

All averaged data are reported ± s.e.m. Statistical comparisons were performed using Microsoft Excel or SPSS 18.0. Tests of independent means were Student's t-test or ANOVA ($\alpha = 0.05$). Tests of repeated measures were paired t-test or MANOVA.

3. Results

The results are in three sections: i) First, we show the results of behavioral training and the location of A1 as determined in post-training mapping experiments. ii) Next, we present a CSD analysis of tone-evoked responses near the 10 kHz CF representation and compare the results to CSD profiles in a more distant representation (~20 kHz CF) in the same animals, and to CSD profiles in untrained controls. iii) Finally, in individual animals we correlate behavioral performance with CSD profiles, to determine whether the physiological changes in A1 could plausibly contribute to learned behavior.

3.1 Behavioral training and tonotopy in A1

Rats (n = 6) were trained to detect a 5 kHz (50 dB SPL) tone in order to receive a food reward, a procedure previously shown to induce plasticity in A1 (Carpenter-Hyland, et al., 2010). Training was repeated for 14 days and performance assessed using d', as previously (Carpenter-Hyland, et al., 2010). For all animals, d' improved over the course of training (Fig. 1; MANOVA, $F_{13,65} = 5.66$, $p < 0.0001$, n = 6), indicating that all animals learned the task.

About 24 h after the 14th and final training session each animal was anesthetized and prepared for electrophysiology. Naive control animals (n = 5) were prepared in the same way. Using tungsten microelectrodes, multiunit recordings from the middle layers were used to map the cortex in ~100–200 μm steps, so as to identify A1 and distinguish it from adjacent fields, especially the ventral auditory field (Fig. 2A; asterisks indicate recording sites in the ventral field) (Polley, Read, Storace, & Merzenich, 2007). At each recording site, frequency-intensity response areas were generated online, and within A1 these generally were V-shaped with clear CFs (Fig. 2B). A1 was identified by short-latency (9–15 ms) responses, well-defined response areas and the expected tonotopic progression of CFs (Polley, et al., 2007; Sally & Kelly, 1988). In each animal we recorded from ~20–35 evenly spaced locations along the long axis of A1 (oriented diagonally in Fig 2A) from regions with CF <4 kHz to CF >32 kHz and including unresponsive areas ("x" in Fig. 2A), in order to establish the extent of A1 and the location within it of regions representing: i) the target

frequency (5 kHz CF), ii) mid-frequency CFs ~10 kHz, and iii) higher-frequency CFs ~20 kHz. Maps were sufficiently dense for this purpose, averaging 26 ± 2.2 recording sites, but we did not attempt to match mapping density among animals or to map the full "width" of A1 (perpendicular to the long axis) in each case, and therefore we did not evaluate the size of CF representations.

3.2 Effects of training on tone-evoked CSD profiles

We then inserted a 16-channel multiprobe at two locations in each animal to measure tone-evoked CSD profiles, first at a mid-frequency site (CF ~10 kHz, range 8–13 kHz) and then at a higher-frequency site (CF ~20 kHz, range 20–23 kHz). At each recording site we determined the response to stimuli over a range of frequencies and intensities in order to determine CF and construct "CSD RFs," i.e., we measured the amplitude of current sinks in different cortical layers evoked over a wide range of frequencies. CF was determined using the shortest-latency middle layer response (a determination that invariably agreed, within ~1 kHz, with CF based on multiunit recordings in approximately the same location during mapping). CF threshold averaged 12.5 ± 1.6 dB SPL and did not differ between mid- and high-frequency sites, or between control and trained animals (range of mean thresholds, 10–14 dB SPL, t-tests, $p > 0.05$).

CF-evoked CSD profiles were similar to those described previously in rodent A1 (Happel, et al., 2010; Intskirveli & Metherate, 2012; Kaur, et al., 2005; H. D. Kawai, et al., 2011), and an example from the mid-frequency site in a trained animal is shown in Fig. 3A. In order to align CSD profiles with cortical layers and average the results across animals, we first identified the shortest-latency current sink in the middle layers (green trace at 600 μm depth in Fig. 3A), which we attributed to thalamocortical input, and assigned this response to mid-layer 4. The remaining CSD traces, recorded at 100 μm intervals, were distributed across layers based on estimated laminar dimensions (Kaur, et al., 2005) (Fig. 3A, numerals designating layers 1–6 are placed at the approximate middle of each layer). We then measured major current sinks, specifically: i) the initial portion of the layer 4 sink (presumed to include thalamocortical input), ii) two sinks located 100 μm and 200 μm more superficially, i.e., within layer 2/3 and possibly upper layer 4 (red traces in Fig. 3A), and iii) a brief and small, but consistent, infragranular sink in layer 5 or 6 (blue trace at 1100 μm in Fig. 3A).

Data from the mid-frequency recording site in trained animals (n = 6, one site per animal) and untrained controls (n = 5) is shown in Fig. 3B–D. The onset of the CF-evoked layer 4 current sink in trained animals averaged 14.5 ± 1.0 ms at a stimulus intensity 20 dB above threshold; onset latencies for the more superficial current sinks were longer than this, but the latency for the infragranular sink did not differ (Fig. 3B, MANOVA, $F_{3,6} = 5.925$; $p = 0.0316$; post-hoc paired t-test: layer 4 vs. layer 2/3 (combined), $p = 0.014$; or vs. +100 μm (as shown), $p = 0.03$, $n = 5$; layer 4 vs. layer 5/6, $p = 0.56$, $n = 5$). A similar analysis in control animals produced similar results (Fig. 3B), i.e., current sinks in layer 4 had shorter onset latencies than in layer 2/3, but not compared to layer 5/6 (paired t-test, CF layer 4 vs. 100 μm above, $p = 0.0016$, $n = 5$; layer 4 vs. 200 μm above, $p = 0.0099$, $n = 5$) These latency differences are consistent with the view that the lemniscal thalamocortical input to layer 4 (with a collateral to layer 5/6) is subsequently relayed intracortically to produce current sinks in layers 2/3 (Douglas & Martin, 1991, 2004; Happel, et al., 2010; Kaur, Lazar, & Metherate, 2004; Kaur, et al., 2005; Liu, Wu, Arbuckle, Tao, & Zhang, 2007; Zhou et al., 2012).

We previously have shown that CF, defined as the stimulus frequency producing the lowest-threshold response (the conventional definition), also is the frequency producing the shortest-latency tone-evoked LFP in layer 4, regardless of intensity (whereas, in contrast,

LFP amplitude does not always indicate CF) (Kaur, et al., 2004). Here we observed a similar finding for CSD profiles: in each cortical layer tested, CF evoked the shortest-latency current sink, whereas progressively higher and lower frequencies produced progressively longer-onset responses. Figure 3C shows this pattern of onset latencies for the current sink in layer 4 and the immediately superficial current sink, for both trained animals and controls. This pattern of onset latencies—longer latencies with increasing spectral distance from CF—has been hypothesized to reflect underlying neural circuitry, with thalamocortical input generating responses to CF and near-CF stimuli, whereas responses to spectrally more-distant stimuli require intracortical relays and associated synaptic delays (Happel, et al., 2010; Kaur, et al., 2004; Kaur, et al., 2005; Metherate, 2011). The results also show that even though onset latencies vary by layer, in each layer tested (layers 2–4) CF elicits the shortest latency response (Fig. 3B, C).

The data in Fig. 3B–C also reveal a result that is important for interpreting training-induced changes in CSD profiles: the inter-laminar latency difference that is apparent at CF disappears with increasing spectral distance from CF. To examine this quantitatively and to increase statistical power, only data up to one octave from CF were considered and frequencies above and below CF were combined since they did not differ (e.g., latencies for CF + 0.25 octave vs. CF − 0.25 octave did not differ, paired t-test, $p > 0.05$, and therefore were combined into a single value for CF ± 0.25 octaves). Similarly, data also were combined from trained animals and controls since they did not differ (t-tests, $p > 0.05$), and the results are shown in Fig. 3D. For the combined data (Fig. 3D), onset latencies differed between layer 4 and the immediately superficial current sink for stimuli up to 0.5 octaves from CF (paired t-tests, $n = 5$: CF, $p = 0.00039$; CF ± 0.25 octaves, $p = 0.00001$; CF ± 0.5 octaves, $p = 0.00047$; all others, $p > 0.05$). These data may reflect the extent to which inputs contributing to tone-evoked responses at CF (presumed thalamocortical inputs) are different than the inputs contributing to responses to stimuli that are spectrally distant from CF. That is, for stimuli within 0.5 octaves of CF, onset latencies in layer 2/3 that are ~2 ms longer than in layer 4 may reflect dependence on an intracortical synaptic relay. At spectral distances greater than 0.5 octaves from CF the onset difference between layers 4 and 2/3 disappears, suggesting that response latencies in both layers reflect intracortical activity; i.e., even latencies in layer 4 are longer than expected for thalamocortical responses, are similar to latencies in layer 2/3, and likely reflect intracortical activity. This difference between response characteristics within CF ± 0.5 octaves vs. outside that range will be used to infer mechanisms of training-induced plasticity (below).

Note that the onset latency data in Fig. 3C for control animals extend to 1.5 octaves below CF, whereas similar measures in trained animals extend to 2.25 octaves below CF. This discrepancy arises because the most spectrally-distant responses in trained animals are not present in controls (or are too small to measure; Fig. 4A). These training-induced responses are detailed next.

To quantify the effects of training on CSD profiles, we constructed CSD RFs by measuring tone-evoked current sinks and their responses to a range of stimulus frequencies: i) to assess thalamocortical input we measured the initial amplitude of the layer 4 current sink, i.e., over its first 3 ms from onset; ii) to assess intracortical activity, we measured the peak amplitude of both current sinks in layer 2/3; and iii) we measured the peak amplitude of the infragranular current sink. The measurements in layers 4 vs. 2/3 differentially reflect thalamocortical vs. intracortical activity, respectively, as shown by recent physiological and pharmacological studies (see Discussion) (Intskirveli & Metherate, 2012; H. Kawai, et al., 2007; H. D. Kawai, et al., 2011). Note that RFs were constructed using stimuli 20 dB above CF threshold, which corresponds to ~30–35 dB SPL. While this value is below that of the training stimulus (50 dB SPL measured at the floor of the testing chamber), a lower intensity

was chosen so that the entire RF width could be measured, and because the variable position of the animal's head and ears during behavior (i.e., typically not facing the overhead speaker directly) would reduce effective stimulus intensities below 50 dB. Thus, the stimulus intensity used for RF testing is likely within the range encountered by the animal during behavioral testing.

CSD RFs for the mid-frequency site are shown in Fig. 4A (for each current sink, RFs were normalized to the largest amplitude response for that animal, and then averaged across animals). For layer 2/3, results did not differ between recording sites 100 μm and 200 μm above layer 4 and are combined. In control animals, the largest amplitude response in each layer typically was to a stimulus near CF, and response amplitudes declined smoothly with increasing spectral distance in either direction. In contrast, trained animals exhibited increased-amplitude current sinks at frequencies below CF, but not at frequencies above CF. For layer 2/3, the current sink in trained animals differed from controls for stimuli below CF (ANOVA, $F = 10.962$, $p = 0.001$), but not for stimuli above CF (ANOVA, $F = 1.115$, $p = 0.344$).

Similar results were obtained in layer 4 for the initial current sink (Fig. 4A, middle). The response in trained animals was greater than in controls for stimuli below CF (ANOVA, $F = 9.451$, $p = 0.001$), but not for stimuli above CF (ANOVA, $F = 1.546$, $p = 0.357$). Note that the enhanced layer 4 response occurs well outside the portion of the receptive field considered to be dependent mainly on direct thalamocortical inputs (gray shading at CF ± 0.5 octaves). The response amplitude of the infragranular current sink was more variable due to its small size, and did not differ between control and trained animals (Fig. 4A, bottom; ANOVA, $F = 0.177$, $p = 0.733$). For post-hoc comparisons, we grouped responses between 1.5 and 2 octaves below CF (location of approximate peak effects) and found differences between control and trained animals in layers 2/3 and 4 (asterisks in Fig. 4A, t-tests: layer 2/3, $p = 0.04$; layer 4, $p = 0.02$, $n = 3–6$).

Because CF at the mid-frequency site ranged from 8–13 kHz, group data explicitly showing the response to the 5 kHz target stimulus are not evident in Fig. 4A (the target stimulus was ~1–1.5 octaves from CF, within the gray hatch patterns in Fig. 4A). Instead, target-evoked group responses are shown in Fig. 4B. The layer 2/3 response to the target stimulus was greater in trained animals than controls (t-test, $p = 0.019$, $n = 5–6$). Neither the layer 4 initial current sink nor the infragranular current sink differed between trained animals and controls in the response to the target stimulus ($p > 0.05$).

Finally, we measured the bandwidth of CSD receptive fields for each group (Fig. 4C; bandwidth at 20 dB above CF threshold estimated by measuring distance from CF, in octaves, of above-baseline evoked responses). Following training, receptive field bandwidth approximately doubled for the current sink in layer 2/3 (t-test, $p = 0.001$, $n = 5–6$). For the initial layer 4 current sink, bandwidth also increased after training (t-test, $p = 0.004$, $n = 5–6$), as did the layer 5/6 bandwidth (t-test, $p < 0.032$, $n = 5–6$).

The results summarized in Fig. 4 indicate that behavioral training exerts a profound effect on CSD profiles in A1 adjacent to the region representing target-frequency CFs. For each animal, we then moved the 16-channel multiprobe to the higher-frequency site (CF ~20 kHz) and again determined CSD RFs 20 dB above threshold. The results are shown in Fig. 5. There was no difference between trained animals and controls for current sink amplitudes in any layer (Fig. 5A, ANOVAs, $p > 0.05$), or for responses to the 5 kHz target frequency (Fig. 5B, $p > 0.05$), or bandwidth 20 dB above threshold (Fig. 5C; $p > 0.05$). Thus, behavioral training with a 5 kHz target did not affect CSD receptive fields in the ~20 kHz CF region of A1.

3.3 Correlation of behavioral performance with CSD profiles

The results thus far indicate that two weeks of training with a 5 kHz target stimulus enhanced intracortical responses to the target frequency at a site in A1 away from the target representation (i.e., at the 10 kHz CF representation; Fig. 4). To determine if there exists a relationship between behavioral performance and target-evoked response amplitudes, we correlated for each animal the amplitude of the 5 kHz-evoked layer 2/3 current sink (same data as in Fig. 4B) with that animal's behavioral performance (d′; same data as in Fig. 1). A d′ value was calculated for each day of training (Days 1–14) whereas physiological data were obtained only once, i.e., one day after training was completed (Day 15).

Figure 6 shows the correlation between d′ on Days 1–14 and the amplitude of the target-evoked current sink in layer 2/3 at the mid-frequency site. Scatter plots (Fig. 6A) show the correlation for each animal on Day 1 of training (correlation coefficient, $r^2 = 0.085$, $p > 0.05$) and on Day 14 ($r^2 = 0.763$, $p < 0.05$). The correlation coefficient calculated for each day generally improved over training (Fig. 6B; dashed line indicates $p = 0.05$). Note that the time course of improvement resembles that of the overall improvement in behavioral performance, and Fig. 6C shows the same graph superimposed on the graph of mean performance from Fig. 1A (both graphs normalized to value at Day 14). As a control, we also correlated d′ with responses to 20 kHz stimuli, i.e., stimuli that are unrelated to training but as spectrally distant as the target frequency from CF at the mid-frequency site (both ~1 octave from CF of 10 kHz). Responses to 20 kHz stimuli did not correlate with performance (r^2 over Days 12–14 averaged 0.1607 ± 0.04, $p > 0.05$). Finally, we correlated d′ with the amplitude of the target-evoked layer 4 initial current sink (same data as in Fig. 4B); interestingly, this correlation was high at the start of training and remained relatively constant across training days, even as group performance improved (r^2 on Days 1–3 = 0.67 ± 0.08, and on Days 12–14 = 0.61 ± 0.09; daily r^2 exceeded significance threshold on 7 of 14 days), possibly indicating relevance of the layer 4 initial sink for behavioral performance, but not learning.

4. Discussion

In this study we used CSD analysis to identify the laminar and spectral profile of learning-induced plasticity in A1. In adult rats, learning to detect a 5 kHz target altered target-evoked CSD profiles in A1 relative to responses in untrained control rats. Training altered CSD RFs in regions of A1 representing a mid-frequency CF (~10 kHz, one octave above the target frequency), but did not change CSD RFs at a more distant site (CF ~20 kHz, two octaves above target). At the mid-frequency site, target-evoked current sinks were enhanced in layer 2/3, but the initial current sink in layer 4 was not affected, and the enhanced responses appeared to involve intracortical circuits. Finally, in individual animals the amplitude of the target-evoked current sink in layer 2/3 correlated strongly with the strength of learning. The results suggest that training-induced plasticity along intracortical pathways in A1 underlies improved performance during learning.

4.1 Interpretation of tone-evoked CSD profiles

A major advantage of the CSD approach is that, ideally, one can simultaneously record inputs to the cortex as well as the cortical response to those inputs. This advantage is important since distinguishing thalamocortical inputs from intracortical responses is difficult even under ideal conditions (e.g., using an *in vitro* thalamocortical slice; Rose and Metherate, 2005). For CF stimuli, several recent studies have examined the contributions of thalamocortical vs. intracortical circuits to evoked CSD profiles. We used the earliest-onset current sink in the middle layers to examine thalamocortical input, which is known to project from the ventral division of the medial geniculate nucleus (MGv) to layer 4 and

lower layer 3 of A1 (Romanski & LeDoux, 1993; Smith, Uhlrich, Manning, & Banks, 2012). Our interpretation is based on studies showing that pharmacological manipulations of thalamus vs. cortex differentially affect the layer 4 initial current sink vs. longer-latency responses in layers 4 and 2/3. Specifically, pharmacological manipulations of the thalamus can reduce the amplitude of the layer 4 current sink (H. Kawai, et al., 2007), or block modulation of the first 3–5 ms of the layer 4 current sink without affecting modulation of peak current sinks in layer 2/3 (Intskirveli & Metherate, 2012). Conversely, intracortical drug treatments, such as intracortical silencing using the GABA-A receptor agonist muscimol, can affect peak current sinks in layers 2–4 without affecting the first 3–5 milliseconds of the layer 4 sink (Happel, et al., 2010; Intskirveli & Metherate, 2012; Kaur, et al., 2004; H. D. Kawai, et al., 2011). These results support the interpretation of CF-evoked CSD profiles used here: the first 3 ms of the layer 4 current sink largely reflects monosynaptic thalamocortical transmission, whereas longer-latency responses in layers 2–4 —in particular, the peak current sink in layer 2/3—largely reflect intracortical contributions. Note that we do not preclude thalamocortical contributions to initial current sinks outside of layer 4, nor intracortical contributions to peak current sinks outside of layer 2/3. Rather, the prior results show that the two measures used in this study—the initial layer 4 sink and the peak layer 2/3 sink—adequately and differentially reflect thalamocortical and intracortical activity, respectively.

In extending this analysis to stimulus frequencies other than CF, a key question is the extent to which the layer 4 initial current sink reflects thalamocortical input to the recording site when activated by stimuli away from CF. Previous studies provide a clear answer for stimuli that are spectrally very distant (2–3 octaves) from CF: intracortical muscimol eliminates those responses indicating their dependence on intracortical pathways (Happel, et al., 2010; Kaur, et al., 2004). However, results for stimuli closer to CF are more difficult to interpret since they can be significantly but not fully reduced by muscimol (Happel, et al., 2010), suggesting partial dependence on intracortical pathways. In the present study we use a complementary approach, asking to what extent the onset of the layer 4 current sink precedes the onset of the layer 2/3 current sink. Since thalamocortical driving of intracortical responses requires a synaptic relay (Douglas & Martin, 1991), the latency difference for CF-evoked response onsets in layer 4 vs. layer 2/3 is evidence for the expected synaptic delay (a recent *in vivo* intracellular study of rat A1 inferred a delay of 2.6 ± 0.7 ms for disynaptic excitation at CF; Zhou, et al., 2012). A timing difference of ~2 ms between sink onsets in layer 4 vs. layer 2/3 occurred for stimuli up to 0.5 octaves from CF (Fig. 3D). However, stimuli that were spectrally more distant elicited current sinks in layers 4 and 2/3 with longer onset latencies that nonetheless were similar to each other, suggesting that neither sink involved direct thalamocortical inputs and both resulted from activity along intracortical pathways. We conclude that stimuli within the range of CF ± 0.5 octaves activate direct thalamocortical inputs to layer 4 at the recording site followed by an intracortical relay to layer 2/3 (and subsequent recurrent excitation of layers 2–4) (Liu, et al., 2007), and stimuli outside of this range activate inputs to the recording site mostly via intracortical pathways throughout layers 2–4. Notably, Kaur et al (2004) reached a similar conclusion following application of muscimol to silence intracortical activity in A1: after muscimol, the spectral width of the remaining (presumed thalamocortical) inputs was ~1 octave or less at 20–30 dB above CF threshold, consistent with the CF ± 0.5 octaves inferred here.

There are several caveats to this interpretation, one being that weak thalamocortical synapses, perhaps at the edge of thalamocortical terminal arbors, could bias rather than drive cortical responses so that evoked responses would not clearly precede intracortical activity. Our criterion must be considered conservative, and weak thalamocortical inputs may be activated by stimuli beyond 0.5 octaves from CF; note, however, that the overall conclusions of our study would not change even if stimuli considerably more distant from CF activated

direct thalamocortical inputs (see next section, below). Also, our conceptual framework does not incorporate nonlemniscal thalamocortical projections to supragranular layers (Cruikshank, Rose, & Metherate, 2002; Herkenham, 1980; Ryugo & Killackey, 1974). Although such inputs might be expected to have longer onset latencies given the spike latencies of some neurons in the nonlemniscal thalamus (Calford, 1983; Calford & Aitkin, 1983) and therefore may not influence the short latency responses analyzed here, it must be recognized that nonlemniscal MG neurons do exhibit learning-induced plasticity (Edeline & Weinberger, 1992) and therefore likely contribute to plasticity in A1. Finally, the infragranular current sink also may reflect thalamocortical (collateral) input (Romanski & LeDoux, 1993; Willard & Ryugo, 1983; Zhou et al., 2010); however, in the present study the infragranular sink was not greatly affected by training.

4.2 Learning-induced plasticity of CSD profiles in the mid-frequency region of A1 is intracortical

A main conclusion of our study is that for the mid-frequency (10 kHz) region of A1 (i.e., distinct from the target 5 kHz representation), training-induced plasticity of CSD RFs involves intracortical synapses in layers 2–4. Conversely, we find no evidence for plasticity of thalamocortical inputs to layer 4 of the 10 kHz region. These data imply that the site of plasticity occurs in one or more of the following: i) in cortico-cortical projections from the target (5 kHz) representation to layers 2–4 of the 10 kHz region; or possibly further "upstream" along ii) thalamocortical projections to layer 4 of the target representation, or iii) local intracortical circuits (e.g., layer 4 to layer 2/3) within the target representation, with changes along (ii) or (iii) subsequently relayed to layers 2–4 of the 10 kHz region. Learning-induced plasticity has been observed in the auditory thalamus, but typically is more prominent, longer-lasting and target-specific in nonlemniscal (MGd, MGm) than in lemniscal (MGv) nuclei (Edeline & Weinberger, 1991, 1992; Ryugo & Weinberger, 1978). Thus, we cannot preclude thalamocortical plasticity, especially from nonlemniscal nuclei that project modulatory excitation to multiple cortical areas.

Our finding of an intracortical origin for altered responses complements previous studies that implicate intracortical mechanisms of adult experience-dependent plasticity (see Introduction), although the prior studies used a variety of behavioral tasks that mostly differed from the tone-detection task used here. Plasticity of tone-evoked unit recordings in A1 likely reflects intracortical responses, at least in part, since action potentials occur at longer latencies than the onsets of LFPs and current sinks (Norena & Eggermont, 2002), and even in layer 4 cannot be attributed solely to thalamocortical inputs. The present results are consistent with mapping studies showing that behavioral training expands the representation of the target stimulus, expressed either as an increased area devoted to the CF representation (Bieszczad & Weinberger, 2010b; Polley, et al., 2006; Recanzone, et al., 1993), or an increase in the area responding to the target itself (Carpenter-Hyland, et al., 2010). The enhanced target-evoked current sinks observed here would be expected to produce increased spike responses, and assuming widespread occurrence should increase the area of A1 responding, as shown (Carpenter-Hyland, et al., 2010). The same synaptic changes would bias unit RFs towards the target frequency, as seen in studies of learning-induced RF plasticity (Bakin & Weinberger, 1990; Fritz, et al., 2003). Finally, if the underlying synapses were strengthened sufficiently, the target stimulus potentially could become CF at the recording site, thereby contributing to the expansion of CF maps (Bieszczad & Weinberger, 2010b; Polley, et al., 2006; Recanzone, et al., 1993). Thus, a variety of previous findings may have resulted from training-induced strengthening of intracortical synapses similar to that described here.

Other approaches provide unambiguous evidence for intracortical plasticity induced by altered behavioral experience, such as the demonstration of postsynaptic expression of the

immediate early gene *Arc* in A1 following the training procedure used here (Carpenter-Hyland, et al., 2010) or, for other sensory cortices, using intracortical stimulation and/or brain slices to isolate cortical synapses, or modifying plasticity via intracortical manipulations (Fox, 2009; Wallace, Glazewski, Liming, & Fox, 2001; Zarzecki et al., 1993). However, while these approaches all implicate intracortical mechanisms, it remains difficult to exclude thalamocortical contributions (Fox, Wallace, & Glazewski, 2002). Therein lies a strength of the CSD approach, i.e., the ability to show unchanged measures of thalamic input at recording sites that show intracortical plasticity.

4.3 Plasticity is not restricted to the target frequency

Perhaps surprisingly, the portion of the CSD RF enhanced by training was not limited to the target frequency, but extended at least 0.5 octaves below the target frequency. This finding does not mean training-induced plasticity was nonselective—for example, plasticity occurred at the mid-frequency site but not at the high-frequency site, and even at the mid-frequency site occurred for stimuli below CF but not above. But clearly, plasticity was not restricted to a narrow range around the target frequency. A possible explanation lies in the nature of the behavioral task, which involved detection of a tone rather than, for example, discrimination among different tones (Polley, et al., 2006; Recanzone, et al., 1993). Given that task demands can determine the specific nature of training-induced plasticity (see Introduction), it is possible that the relatively broad enhancement of CSD RFs near the target frequency reflects the lesser importance in this task of the specific frequency used. More restricted plasticity may occur during tone discrimination training. Alternatively, or in addition, an early phase of learning-induced plasticity may appear nonselective in that it is not closely related to the target frequency, as seen previously with this task (Carpenter-Hyland, et al., 2010). A nonselective phase of plasticity has been found in multiple studies of operant sensory learning in nonhuman primates (Blake, Heiser, Caywood, & Merzenich, 2006; Blake, Strata, Churchland, & Merzenich, 2002; Blake, Strata, Kempter, & Merzenich, 2005). It is possible that nonselective enhanced responsiveness serves to unmask subthreshold responses and allow for subsequent selective reinforcement of target responses. The relatively selective changes observed in the present study may reflect an intermediate phase of plasticity, prior to the emergence of target-specific changes.

4.4 Function of intracortical plasticity in A1

A second major finding is that the amplitudes of target-evoked, layer 2/3 intracortical responses at the mid-frequency site correlate with behavioral performance (Fig. 6); e.g., better learners have larger evoked responses. The evoked response measured after training (on Day 15) correlated with behavior at the end of training but not at the beginning, implying that the increased correlation over training links intracortical plasticity to learning. Conversely, stimuli unrelated to the target (e.g., 20 kHz, which like the target is ~1 octave from the mid-frequency CF but in the opposite direction) produced response amplitudes that did not correlate with performance. Target-evoked responses in layer 4 also correlated with behavior, but interestingly, this correlation was relatively constant throughout training. Since layer 2/3 target-evoked responses exhibit training-induced plasticity whereas layer 4 responses do not (Fig. 4B), we speculate that the layer 4 response may be related to performance, but not learning, throughout training, whereas intracortical plasticity in layer 2/3 is related to the improvement in performance over training, i.e., learning. Note that sound-evoked cortical responses normally may be necessary for hearing, since tone-detection ability on an appetitive operant conditioning task is lost following cortical silencing with muscimol (Talwar, Musial, & Gerstein, 2001).

The finding that better learners exhibit greater intracortical plasticity is likely related to earlier observations that better learning is associated with increased representational area in

A1 (Bieszczad & Weinberger, 2010b; Polley, et al., 2006; Recanzone, et al., 1993; Rutkowski & Weinberger, 2005). Note, however, that studies have reported learning without cortical map plasticity (Brown, et al., 2004) (although the latter reports a trend towards increased RF bandwidth for multiunit clusters with CF near the target frequency), or cortical plasticity that is related to some but not all measures of learned behavior (Edeline & Weinberger, 1993). Our conclusions also are reminiscent of recent studies of cholinergic function in the auditory forebrain, showing that better learners have more robust nicotinic regulation of tone-evoked responses (Bieszczad et al., 2012; Liang, Poytress, Weinberger, & Metherate, 2008). It is possible that better learning is associated with stronger activation of attention-related acetylcholine systems, with resultant cholinergic plasticity of auditory-evoked responses in layer 2/3. Future studies will focus on these systems, both auditory and cholinergic, and their interactions to better understand mechanisms of learning-induced plasticity.

Acknowledgments

We thank Dr. Tom Lu of the Computing and Engineering Core, Center for Hearing Research, for CSD analysis software, and Ronit Lazar for assistance with behavioral training. This research was supported by NIH grants (R01 DA12929 and P30 DC08369) to RM and by fellowship awards to FG from the China Scholarship Council and the UC Irvine Center for the Neurobiology of Learning and Memory.

References

Bakin JS, Weinberger NM. Classical conditioning induces CS-specific receptive field plasticity in the auditory cortex of the guinea pig. Brain Res. 1990; 536:271–286. [PubMed: 2085753]

Bieszczad KM, Kant R, Constantinescu CC, Pandey SK, Kawai HD, Metherate R, Weinberger NM, Mukherjee J. Nicotinic acetylcholine receptors in rat forebrain that bind (1)(8)F-nifene: relating PET imaging, autoradiography, and behavior. Synapse. 2012; 66(5):418–434. [PubMed: 22213342]

Bieszczad KM, Weinberger NM. Learning strategy trumps motivational level in determining learning-induced auditory cortical plasticity. Neurobiol Learn Mem. 2010a; 93(2):229–239. [PubMed: 19853056]

Bieszczad KM, Weinberger NM. Representational gain in cortical area underlies increase of memory strength. Proc Natl Acad Sci U S A. 2010b; 107(8):3793–3798. [PubMed: 20133679]

Blake DT, Heiser MA, Caywood M, Merzenich MM. Experience-dependent adult cortical plasticity requires cognitive association between sensation and reward. Neuron. 2006; 52(2):371–381. [PubMed: 17046698]

Blake DT, Strata F, Churchland AK, Merzenich MM. Neural correlates of instrumental learning in primary auditory cortex. Proc Natl Acad Sci U S A. 2002; 99(15):10114–10119. [PubMed: 12119383]

Blake DT, Strata F, Kempter R, Merzenich MM. Experience-dependent plasticity in S1 caused by noncoincident inputs. J Neurophysiol. 2005; 94(3):2239–2250. [PubMed: 16105958]

Brown M, Irvine DR, Park VN. Perceptual learning on an auditory frequency discrimination task by cats: association with changes in primary auditory cortex. Cereb Cortex. 2004; 14(9):952–965. [PubMed: 15115736]

Calford MB. The parcellation of the medial geniculate body of the cat defined by the auditory response properties of single units. J Neurosci. 1983; 3(11):2350–2364. [PubMed: 6631485]

Calford MB, Aitkin LM. Ascending projections to the medial geniculate body of the cat: evidence for multiple, parallel auditory pathways through thalamus. J Neurosci. 1983; 3(11):2365–2380. [PubMed: 6313877]

Carpenter-Hyland EP, Plummer TK, Vazdarjanova A, Blake DT. Arc expression and neuroplasticity in primary auditory cortex during initial learning are inversely related to neural activity. Proc Natl Acad Sci U S A. 2010; 107(33):14828–14832. [PubMed: 20675582]

Cruikshank SJ, Rose HJ, Metherate R. Auditory thalamocortical synaptic transmission in vitro. J Neurophysiol. 2002; 87(1):361–384. [PubMed: 11784756]

Douglas RJ, Martin KA. A functional microcircuit for cat visual cortex. J Physiol. 1991; 440:735–769. [PubMed: 1666655]

Douglas RJ, Martin KA. Neuronal circuits of the neocortex. Annu Rev Neurosci. 2004; 27:419–451. [PubMed: 15217339]

Edeline JM. The thalamo-cortical auditory receptive fields: regulation by the states of vigilance, learning and the neuromodulatory systems. Exp Brain Res. 2003; 153(4):554–572. [PubMed: 14517594]

Edeline JM, Weinberger NM. Thalamic short term plasticity in the auditory system: associative retuning of receptive fields in the ventral medial geniculate body. Behav Neurosci. 1991; 105(5): 618–639. [PubMed: 1815615]

Edeline JM, Weinberger NM. Associative retuning in the thalamic source of input to the amygdala and auditory cortex: receptive field plasticity in the medial division of the medial geniculate body. Behav Neurosci. 1992; 106(1):81–105. [PubMed: 1554440]

Edeline JM, Weinberger NM. Receptive field plasticity in the auditory cortex during frequency discrimination training: selective retuning independent of task difficulty. Behav Neurosci. 1993; 107(1):82–103. [PubMed: 8447960]

Fox K. Experience-dependent plasticity mechanisms for neural rehabilitation in somatosensory cortex. Philos Trans R Soc Lond B Biol Sci. 2009; 364(1515):369–381. [PubMed: 19038777]

Fox K, Wallace H, Glazewski S. Is there a thalamic component to experience-dependent cortical plasticity? Philos Trans R Soc Lond B Biol Sci. 2002; 357(1428):1709–1715. [PubMed: 12626005]

Fritz J, Elhilali M, Shamma S. Active listening: task-dependent plasticity of spectrotemporal receptive fields in primary auditory cortex. Hear Res. 2005; 206(1–2):159–176. [PubMed: 16081006]

Fritz J, Shamma S, Elhilali M, Klein D. Rapid task-related plasticity of spectrotemporal receptive fields in primary auditory cortex. Nat Neurosci. 2003; 6(11):1216–1223. [PubMed: 14583754]

Guo F, Zhang J, Zhu X, Cai R, Zhou X, Sun X. Auditory discrimination training rescues developmentally degraded directional selectivity and restores mature expression of GABA(A) and AMPA receptor subunits in rat auditory cortex. Behav Brain Res. 2012; 229(2):301–307. [PubMed: 22306199]

Happel MF, Jeschke M, Ohl FW. Spectral integration in primary auditory cortex attributable to temporally precise convergence of thalamocortical and intracortical input. J Neurosci. 2010; 30(33):11114–11127. [PubMed: 20720119]

Herkenham M. Laminar organization of thalamic projections to the rat neocortex. Science. 1980; 207:532–535. [PubMed: 7352263]

Intskirveli I, Metherate R. Nicotinic neuromodulation in auditory cortex requires MAPK activation in thalamocortical and intracortical circuits. J Neurophysiol. 2012; 107:2782–2793. [PubMed: 22357798]

Irvine DR. Auditory cortical plasticity: does it provide evidence for cognitive processing in the auditory cortex? Hear Res. 2007; 229(1–2):158–170. [PubMed: 17303356]

Kaur S, Lazar R, Metherate R. Intracortical pathways determine breadth of subthreshold frequency receptive fields in primary auditory cortex. J Neurophysiol. 2004; 91(6):2551–2567. [PubMed: 14749307]

Kaur S, Rose HJ, Lazar R, Liang K, Metherate R. Spectral integration in primary auditory cortex: laminar processing of afferent input, in vivo and in vitro. Neuroscience. 2005; 134:1033–1045. [PubMed: 15979241]

Kawai H, Lazar R, Metherate R. Nicotinic control of axon excitability regulates thalamocortical transmission. Nat Neurosci. 2007; 10(9):1168–1175. [PubMed: 17704774]

Kawai HD, Kang HA, Metherate R. Heightened nicotinic regulation of auditory cortex during adolescence. J Neurosci. 2011; 31(40):14367–14377. [PubMed: 21976522]

Liang K, Poytress BS, Weinberger NM, Metherate R. Nicotinic modulation of tone-evoked responses in auditory cortex reflects the strength of prior auditory learning. Neurobiol Learn Mem. 2008; 90(1):138–146. [PubMed: 18378471]

Liu BH, Wu GK, Arbuckle R, Tao HW, Zhang LI. Defining cortical frequency tuning with recurrent excitatory circuitry. Nat Neurosci. 2007; 10(12):1594–1600. [PubMed: 17994013]

Ma X, Suga N. Specific and nonspecific plasticity of the primary auditory cortex elicited by thalamic auditory neurons. J Neurosci. 2009; 29(15):4888–4896. [PubMed: 19369557]

Metherate R. Functional connectivity and cholinergic modulation in auditory cortex. Neurosci Biobehav Rev. 2011; 35(10):2058–2063. [PubMed: 21144860]

Muller-Preuss P, Mitzdorf U. Functional anatomy of the inferior colliculus and the auditory cortex: current source density analyses of click-evoked potentials. Hear Res. 1984; 16:133–142. [PubMed: 6526745]

Norena A, Eggermont JJ. Comparison between local field potentials and unit cluster activity in primary auditory cortex and anterior auditory field in the cat. Hear Res. 2002; 166(1–2):202–213. [PubMed: 12062772]

Polley DB, Read HL, Storace DA, Merzenich MM. Multiparametric auditory receptive field organization across five cortical fields in the albino rat. J Neurophysiol. 2007; 97(5):3621–3638. [PubMed: 17376842]

Polley DB, Steinberg EE, Merzenich MM. Perceptual learning directs auditory cortical map reorganization through top-down influences. J Neurosci. 2006; 26(18):4970–4982. [PubMed: 16672673]

Recanzone GH, Schreiner CE, Merzenich MM. Plasticity in the frequency representation of primary auditory cortex following discrimination training in adult owl monkeys. J Neurosci. 1993; 13(1): 87–103. [PubMed: 8423485]

Romanski LM, LeDoux JE. Organization of rodent auditory cortex: anterograde transport of PHA-L from MGv to temporal neocortex. Cereb Cortex. 1993; 3(6):499–514. [PubMed: 7511011]

Rose HJ, Metherate R. Auditory thalamocortical transmission is reliable and temporally precise. J Neurophysiol. 2005; 94:2019–2030. [PubMed: 15928054]

Rutkowski RG, Weinberger NM. Encoding of learned importance of sound by magnitude of representational area in primary auditory cortex. Proc Natl Acad Sci U S A. 2005; 102(38):13664–13669. [PubMed: 16174754]

Ryugo DK, Killackey HP. Differential telencephalic projections of the medial and ventral divisions of the medial geniculate body of the rat. Brain Res. 1974; 82:173–177. [PubMed: 4611594]

Ryugo DK, Weinberger NM. Differential plasticity of morphologically distinct neuron populations in the medical geniculate body of the cat during classical conditioning. Behav Biol. 1978; 22(3):275–301. [PubMed: 626625]

Sally SL, Kelly JB. Organization of auditory cortex in the albino rat: sound frequency. J Neurophysiol. 1988; 59:1627–1638. [PubMed: 3385476]

Scheich H, Brechmann A, Brosch M, Budinger E, Ohl FW. The cognitive auditory cortex: task-specificity of stimulus representations. Hear Res. 2007; 229(1–2):213–224. [PubMed: 17368987]

Smith PH, Uhlrich DJ, Manning KA, Banks MI. Thalamocortical projections to rat auditory cortex from the ventral and dorsal divisions of the medial geniculate nucleus. J Comp Neurol. 2012; 520(1):34–51. [PubMed: 21618239]

Talwar SK, Musial PG, Gerstein GL. Role of mammalian auditory cortex in the perception of elementary sound properties. J Neurophysiol. 2001; 85(6):2350–2358. [PubMed: 11387381]

Wallace H, Glazewski S, Liming K, Fox K. The role of cortical activity in experience-dependent potentiation and depression of sensory responses in rat barrel cortex. J Neurosci. 2001; 21(11): 3881–3894. [PubMed: 11356876]

Weinberger NM. Associative representational plasticity in the auditory cortex: a synthesis of two disciplines. Learn Mem. 2007; 14(1–2):1–16. [PubMed: 17202426]

Willard, FH.; Ryugo, DK. Anatomy of the central auditory system. In: Willott, JF., editor. The Auditory Psychobiology of the Mouse. Springfield: Charles C. Thomas; 1983. p. 201-304.

Zarzecki P, Witte S, Smits E, Gordon DC, Kirchberger P, Rasmusson DD. Synaptic mechanisms of cortical representational plasticity: somatosensory and corticocortical EPSPs in reorganized raccoon SI cortex. J Neurophysiol. 1993; 69(5):1422–1432. [PubMed: 8509825]

Zhou Y, Liu BH, Wu GK, Kim YJ, Xiao Z, Tao HW, Zhang LI. Preceding inhibition silences layer 6 neurons in auditory cortex. Neuron. 2010; 65(5):706–717. [PubMed: 20223205]

Zhou Y, Mesik L, Sun YJ, Liang F, Xiao Z, Tao HW, Zhang LI. Generation of spike latency tuning by thalamocortical circuits in auditory cortex. J Neurosci. 2012; 32(29):9969–9980. [PubMed: 22815511]

Highlights

1. We trained adult rats to detect a 5 kHz target tone to receive a food reward.
2. Training altered target-evoked CSD profiles at the 10 kHz site in A1.
3. Target-evoked responses were enhanced in layer 2/3 but not layer 4.
4. Each rat's performance correlated with amplitude of target-evoked current sink.
5. We conclude that plasticity along intracortical pathways is important for auditory learning.

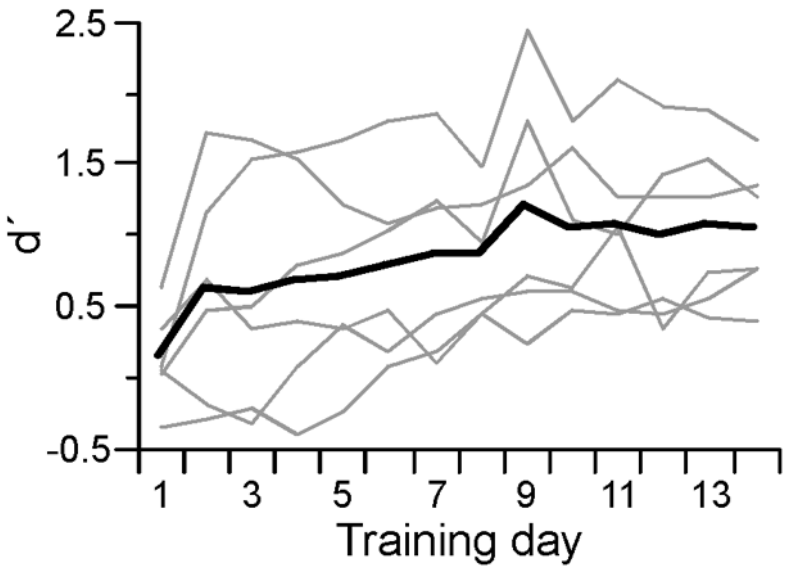

Fig. 1.
Behavioral performance of trained animals. Performance (d′) for individual rats (gray lines, n = 6) and group average (black line) over Days 1–14 of acoustic training.

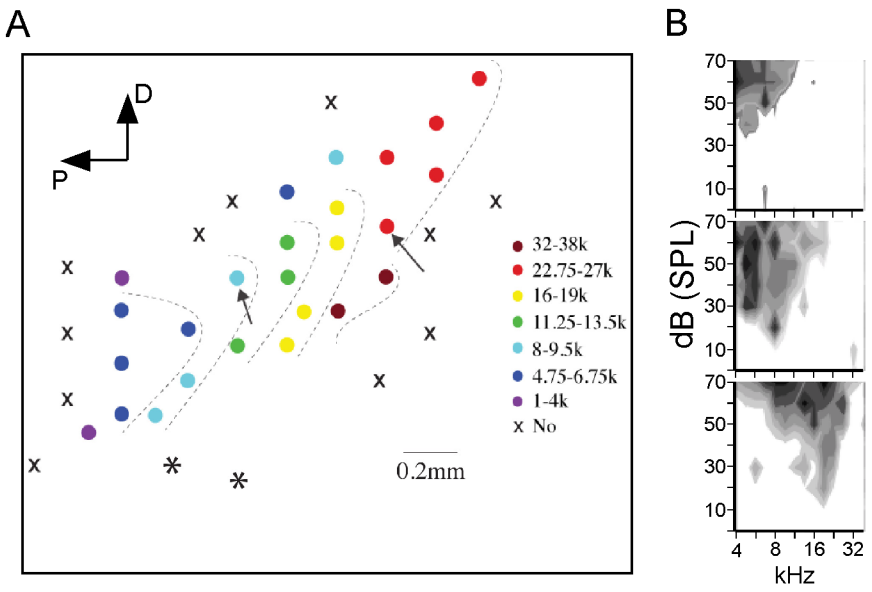

Fig. 2.

Identifying A1 and determining the location of a mid-frequency and a high-frequency CF site for CSD profiles. (A) Example of tonotopic progression of CF used to identify A1 in a trained animal. Circles represent recording sites color coded by CF; 'X' symbols indicate no response; asterisks indicate high-frequency CFs that do not fall in the tonotopic progression expected for A1, and therefore indicate sites in the ventral auditory field (Polley, et al., 2007). Arrows indicate location of subsequent multiprobe recordings for determining CSD RFs. D, dorsal; P, posterior. (B) Three examples of response areas determined online during mapping procedure and used to determine CF. Gray shading indicates multiunit response magnitude; darker shading indicates greater magnitude.

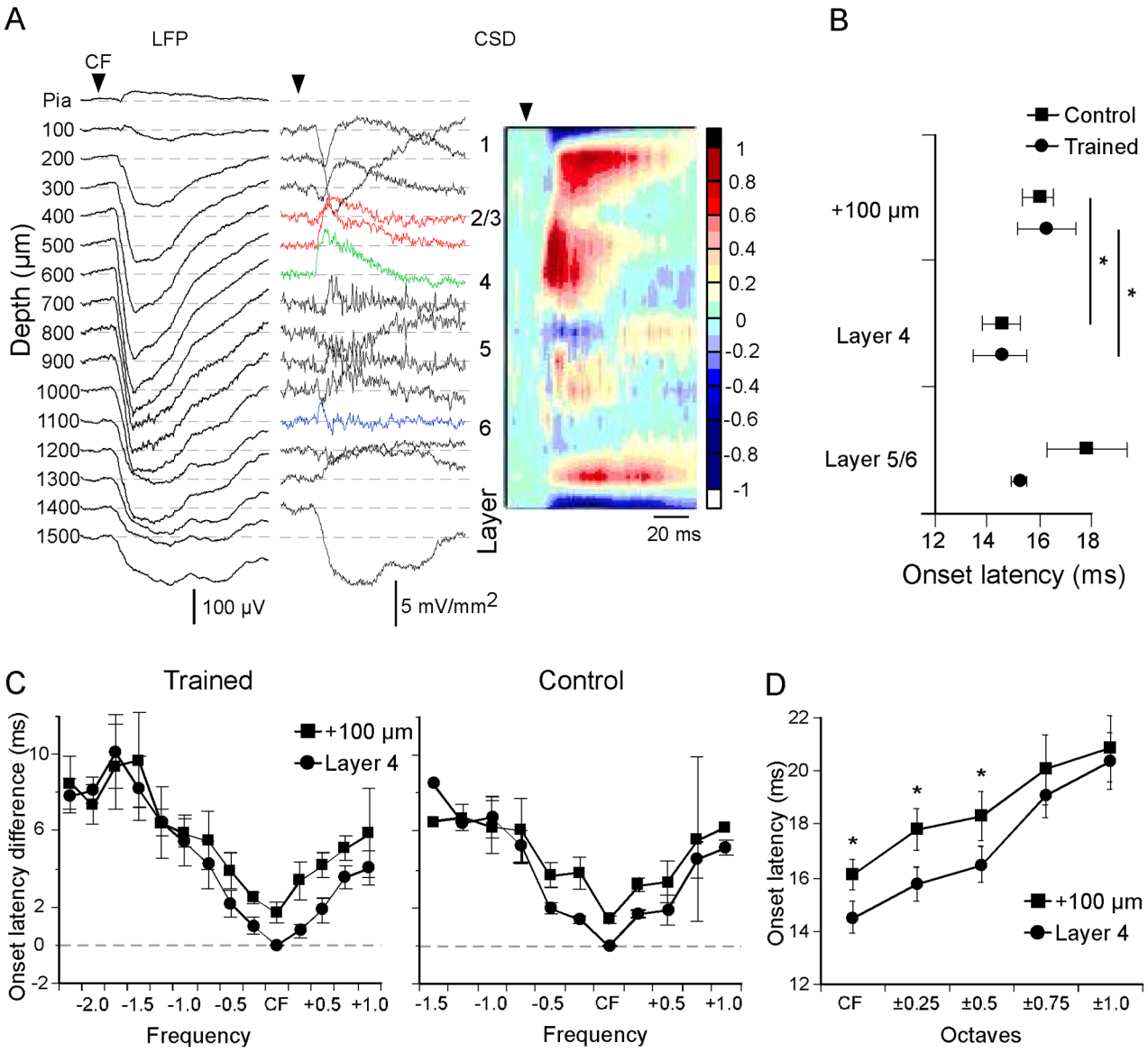

Fig. 3.

Laminar and spectral profile of current sink onset latencies. (A) Example of CF-evoked LFPs recorded using a 16-channel multiprobe (left column), derived one-dimensional CSD traces (middle) and interpolated CSD profile (right) (CF stimulus: 11.25 kHz, 50 dB SPL, 100 ms). Color scale indicates response amplitudes normalized to the largest current sink (reds) and source (blues). (B) Mean CF-evoked onset latencies for three major current sinks in trained animals and controls. (C) Spectral profile of current sink onset latencies relative to CF-evoked onset in layer 4 in trained animals (left) and naive control animals (right). (D) Comparison of current sink onset latencies in layer 4 vs. 100 μm above with increasing spectral distance from CF (data combined from positive and negative spectral distance, and from trained animals and controls). In B-D, data derive from mid-frequency recordings sites (one per animal; n = 6 for trained animals, n = 5 for controls). * $p < 0.05$.

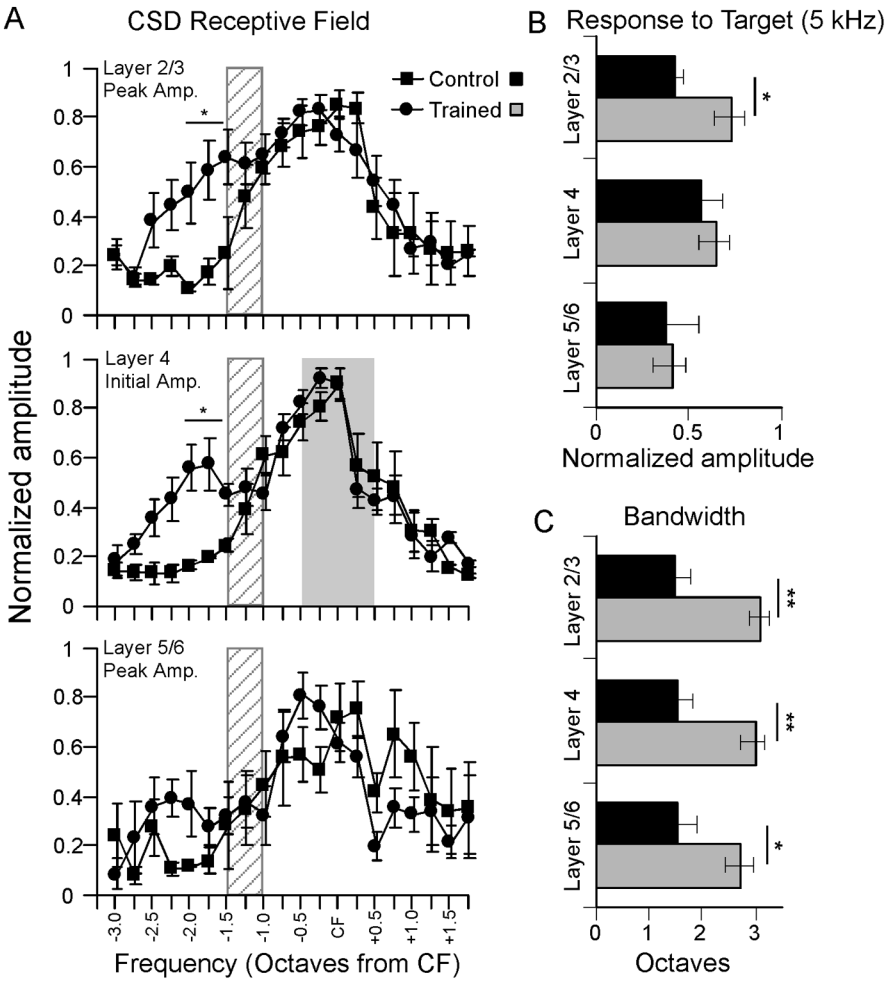

Fig. 4.

Mean CSD RFs at mid-frequency recording site (CF range, 8–13 kHz) in trained animals (n = 6) and untrained controls (n = 5). (A) CSD RFs for current sink peak amplitude in layer 2/3 (top), current sink initial amplitude in layer 4 (middle) and current sink peak amplitude in layer 5/6 (bottom). RFs obtained 20 dB above CF threshold; hatch pattern 1–1.5 octaves from CF on each graph indicate approximate location of target frequency, and gray shading in the middle graph indicates the estimated extent of thalamocortical inputs to layer 4 (CF ± 0.5 octaves,). (B) Amplitude of 5 kHz-evoked current sink in each layer (same data as in A, rearranged). (C) Bandwidth of current sink RFs in A. * $p < 0.05$, ** $p < 0.01$

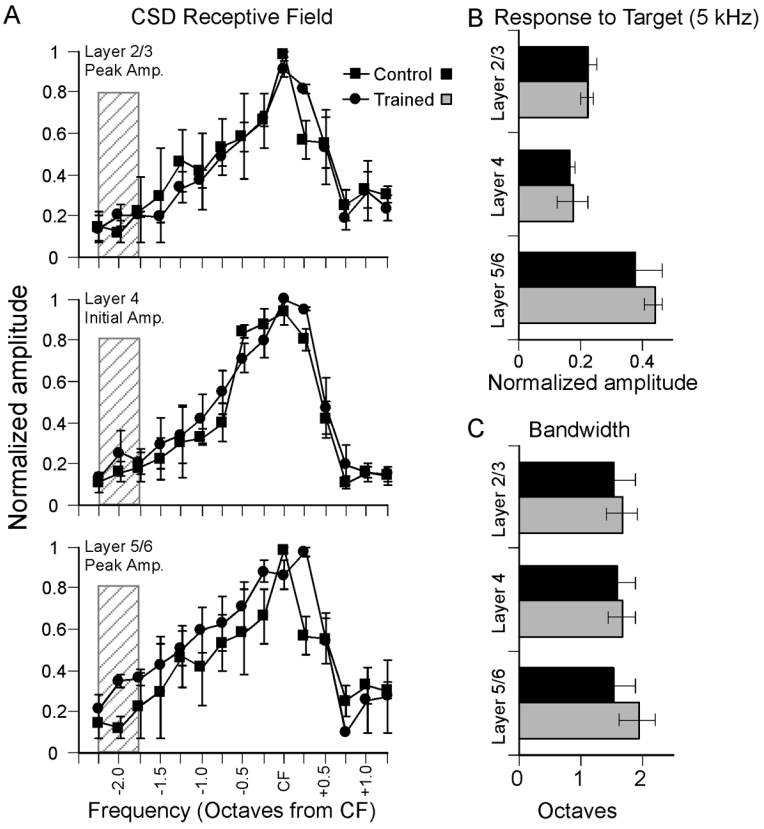

Fig. 5.

Mean CSD RFs at high-frequency recording site (CF range, 20–23 kHz) for same animals as in Fig. 4. (A) CSD RFs for current sink peak amplitude in layer 2/3 (top), current sink initial amplitude in layer 4 (middle) and current sink peak amplitude in layer 5/6 (bottom). RFs obtained 20 dB above CF threshold; hatch pattern indicate approximate location of target frequency (1.75–2.25 octaves from CF). (B) Amplitude of 5 kHz-evoked current sink in each layer (same data as in A, rearranged). (C) Bandwidth of RFs in A.

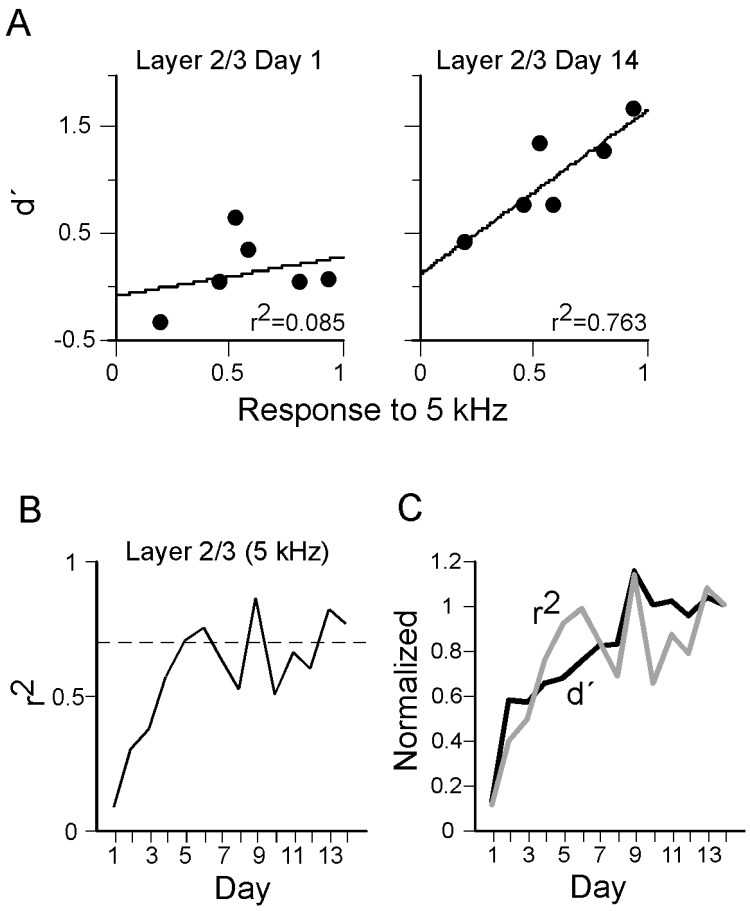

Fig. 6.

Correlation of behavioral performance with target-evoked current sink amplitudes in layer 2/3 in individual animals. Behavioral data obtained during training Days 1–14, physiological data obtained on Day 15 from mid-frequency recording site. (A) Scatter plots show correlation of d′ on the first and last days of training with the normalized amplitude of the target-evoked current sink peak in layer 2/3. (B) Change in correlation coefficient using behavioral data from each day of training. (C) Superimposed graphs from B and from Fig. 1A.